Introduction to track structure and z*2/β2. Curtis SB. https://three.jsc.nasa.gov/articles/Track-Structure-SCurtis.pdf.
Date Posted: 02-29-2016

INTRODUCTION TO TRACK STRUCTURE AND z^{*2}/β^2

Stanley B. Curtis (ret.)
Fred Hutchinson Cancer Research Center
University of Washington
Seattle, WA

Abstract

The spatial distributions of radiation deposition created by the galactic cosmic rays (GCR) traversing the bodies of space travelers on missions outside the magnetosphere are very different from those caused by x-rays and gamma rays, the radiations of most concern here on Earth. Although both are caused by electrons of various energies, the spatial distributions of the energy depositions around the GCR tracks are unique to the charge and velocity of the incident particles. They are dense around the track trajectory and drop off roughly as the inverse square of the distance from the trajectory. Thus it is not surprising that they might cause different amounts of biological damage than electron energy depositions more uniformly distributed by conventional radiations. Here we introduce particle *fluence* as the important physical parameter of the incident radiation, show its relationship to absorbed dose, and develop in a non-relativistic semi-quantitative way the spatial distribution characteristics of energy depositions of the particles as they slow down. This leads to the emergence of the quantity, z^{*2}/β^2, (where z^* and β are proportional to the charge and velocity of the particle, respectively) as a descriptor of biological damage. It has been shown experimentally in some instances to be a better quantitative descriptor than LET_∞ (the total energy lost per unit track length). It is proportional to the number of electrons emitted per unit track length. The stochastic nature of the energy loss process is also introduced and Monte Carlo generated tracks are presented to show the vastly different track structures of various components of the GCR (e.g., He and Fe tracks) at the same LET_∞. These considerations of the importance of track structure have been taken into account in the development of the present NASA Radiation Risk Model (Cucinotta *et al.*, 2013).

Preface

The field of radiation track structure is important in the area of space radiation risk analysis because of the very different manner in which energy in the radiation found in space is deposited in the bodies of space travelers compared to the way it is deposited by radiations of importance on Earth. Although electrons play the major role in each situation, both the *spatial and temporal distribution* of the electrons are critical in determining biological response. This was recognized early in the Space Age in a report of an advisory panel of the National Academy of Sciences (NAS, 1973). Because of this importance, several articles in THREE have been dedicated to the description of the unique manner in which the charged particles found in space (high energy protons, helium ions and HZE particles) lose their energy in the bodies of space travelers. Other articles of interest in this regard are (Curtis, 2013), (Dicello & Cucinotta, 2012), (Braby, 2014), (Toburen, 2014), (Dingfelder, 2014) and will be referred to in appropriate places in the present article.

1.0 What is Track Structure?

Track structure relates to the manner or pattern in which energy is deposited in a medium (for example, an astronaut's body) by tracks of charged particles as they slow down. The mean rate of energy lost by a charged particle per unit track length (the linear energy transfer or LET_∞) depends on such physical quantities as its mass, velocity and charge. At the same LET_∞, however, different particles (e.g., protons, He, Ne, and Fe ions) have different patterns of energy deposition, i.e., different track structure. In general, at the same LET_∞, heavier and more highly charged particles are higher in velocity (and energy) and produce higher energy electrons and so spread out their energy loss to greater distances around the track than lighter lower charged particles. The radiation within space travelers will consist mainly of individual high-energy charged particles (primaries and secondaries) from galactic cosmic rays and sporadically from solar particles, which are mostly protons. It is important to determine differences, if any, in the biological effects caused by various particle types at the same LET_∞, since space radiation risk has traditionally been calculated by using a Quality Factor, which depends only on the particle's LET_∞, and such calculated risks may be in error if different particles with the same LET_∞ cause different amounts or types of biological effects due to their differences in track structure.

1.1 Fluence and Delta Rays

The fluence, ϕ, of particles passing through a volume is the number of particles through the volume divided by the area subtended by the volume and has the dimension of number per unit area. In the *continuously slowing down approximation* (*csda*) and under secondary particle equilibrium, the energy ΔE deposited in a small volume, $\Delta V = \Delta x \Delta A$, of tissue within a space traveler is given by the number of particles passing through the volume, (i.e., the product of the fluence ϕ and the area ΔA subtended, $\phi \Delta A$) times the average energy deposited by a particle passing through the volume (i.e., the LET_∞, L, times the track length through the volume, $L\Delta x$). The absorbed dose, D, in the volume is defined as the average (or mean) energy, ΔE, deposited by this fluence divided by the mass of the volume, Δm, which is the product of the volume, ΔV, and its density, ρ. Therefore, we have the well-known expression for the absorbed dose, D:

$$D = \frac{\Delta E}{\Delta m} = \frac{\phi \Delta A L \Delta x}{\rho \Delta V} = \frac{\phi L}{\rho} \qquad (1)$$

Delta rays are electrons knocked out of the atoms of the medium by the process of ionization. Traditionally, a minimum energy of around 100 eV was required in this definition for them to produce their own "tracks" in a detector. The emission is caused by an electromagnetic interaction of the charge of the particle with the charge of an orbital electron, the subsequent ejection of the electron, and loss of energy of the charged particle. Depending on their energy, these delta rays in tissue can have rather large ranges and can travel distances on the order of the size of biological cells (i.e., several micrometers) or more, even up to many millimeters for the highest energy deltas. It is the wanderings (scattering) of these electrons (and the secondary electrons they produce) and how their numbers and energy-deposits spread from the track trajectory that make up the pattern of energy depositions that we call *track structure*.

2.0 Stochastic Effects

The energy transfers responsible for the slowing down of the particle, however, occur randomly along the track. The positions of the transfers are not predictable and in any extremely small volume, there may or may not be a deposition of energy by the particle or one (or more) of the delta rays. This process of randomness in the energy loss is called a *stochastic* process. Thus, any given small biological target or detector may or may not experience an energy-loss event. This has led to the development of a branch of *microdosimetry*, which is the study of the stochastic nature of the energy loss process and the measurement of the distribution of energy losses in appropriate detectors. More on this approach to microdosimetry can be found in the articles in THREE by (Braby, 2014), and (Dicello & Cucinotta, 2012). A realistic way of taking the stochastic nature of the energy loss processes into account in calculating pictorial representations of tracks is by using the Monte Carlo (i.e., probabilistic) procedure. A history of the Monte Carlo approach for calculating heavy ion tracks can be found in the article by (Toburen, 2014), and the task of calculating tracks by this method is described in some detail in the article by (Dingfelder, 2014). A comparison of two tracks (a helium ion and an iron ion) at the same LET is presented in Section 5.0 of the present article for a visual comparison of their track structures in the size range typical of a biological cell.

3.0 Early work on Energy Loss, z^{*2}/β^2, and Radial Dose from Heavy Charged Particles

The LET_∞ or dE/dx of a charged particle varies approximately as z^2/β^2 where z is the particle's charge (relative to that of the proton) and β is the ratio of the particle's velocity to that of light in vacuum. In early models of track structure, the energy deposition pattern around the track trajectory was considered as consisting of a "core" and a "penumbra". The energy deposited in the "core" (i.e., close to the trajectory) was from ionizations, excitations and collective oscillations of the atoms of the medium from so-called "close" collisions (i.e., "hard" collisions with the atomic electrons and atom as a whole). The energy deposited in the "penumbra" was from the atomic electrons (from both "close and "glancing" collisions). The maximum energy transferable to an electron depends on the energy and mass of the incident charged particle and can be calculated by applying principles of conservation of energy and

momentum in a collision with the electron considered at rest. It is now accepted that a majority of the energy (~85% – 95%) goes into these delta rays and about 5% – 15% into excitation and collective oscillations of the atoms (Cucinotta, Nikjoo, Goodhead, 1999).

3.1 A Classical Development of the Rutherford Expression for Electron Emission and the Emergence of z^{*2}/β^2 as a Possible Physical Descriptor of Biological Effect instead of LET

We begin by considering[1] a heavy totally ionized particle (as heavy as or heavier than a proton) of charge *ze* and velocity *v (= βc)* and mass *m*, encountering an atom (or molecule) in a stopping medium of atomic number Z and atomic mass A. Here *z* is the charge number of the particle, *e* is the protonic charge, and *c* is the velocity of light in vacuum. The particle will interact electrically with the electrons of the atoms in the medium, imparting to them enough energy to escape their orbits around the nucleus and become free electrons, i.e., delta rays. It will also interact with the nucleus, but since the nucleus is so much heavier than the electrons, the mean energy transferred to it is negligible compared to that transferred to the electrons and can be neglected here. We consider only small momentum transfers between the two particles, and neglect the motion and binding energy of the target electron during the interaction; that is, the electron is considered free and at rest. Let *b* be the *impact parameter*, i.e., the distance of the trajectory of the incident particle from the electron before the encounter. Under the assumptions made, *b* represents the minimum distance of approach between the two particles. The force between them reaches its maximum at the moment of closest approach. Ignoring relativistic deformation of the field for the moment, the maximum value of the force on the electron is:

$$f = ze^2/b^2 \qquad (2)$$

We will carry out here the computation of the momentum transferred from the particle to the electron as the particle passes (i.e., the *impulse* given to the electron) in a semi-quantitative way, which brings out the significant physical features. The "collision time", τ, during which the value of the force is of the same *order of magnitude* as the maximum value given by Eq. 2 (say greater than *f/2*) is:

$$\tau = 2b/\beta c \qquad (3)$$

So the electron acquires an impulse or momentum *Δp* on the order of:

$$\Delta p = f \cdot \tau = \frac{ze^2}{b^2}\,\frac{2b}{\beta c} = \frac{2ze^2}{b\beta c} \qquad (4)$$

In the case of relativistic velocity of the incident particle, the maximum value of the force *f* is increased by a factor $\gamma = 1/\sqrt{1-\beta^2}$ while the "collision time" τ decreases by the reciprocal of the same factor. Thus the product $f{\cdot}\tau$ remains unchanged.

[1] This section follows a development of the classical derivation of the Rutherford scattering formula given in Rossi, 1952.

Making the assumption that the kinetic energy, *w*, acquired by the electron of mass m_e is small compared to its rest energy, $m_e c^2$, the electron energy can be computed from the nonrelativistic relation between kinetic energy and momentum:

$$w = \frac{(\Delta p)^2}{2m_e} = \frac{2z^2 e^4}{m_e c^2 b^2 \beta^2} \tag{5}$$

This can be rewritten in terms of the *classical radius of the electron* ($r_e = e^2/m_e c^2$):

$$w = 2m_e c^2 \frac{z^2 r_e^2}{\beta^2 b^2} \tag{6}$$

The probability *dn(w)* of an energy transfer to an electron in *dw* at *w* in a given thickness of material *dx* g cm^{-2} is equal to the probability *F(b)* of a collision with impact parameter in *db* at *b*, where *w* and *b* are related by Eq. 6. The probability of a collision *F(b)* with impact parameter in *db* at *b* in a thickness of *dx* g cm^{-2} is given by considering a cylindrical shell of radius *b* and thickness *db* around the trajectory. The above equality is related by:

$$dn(w)dx = F(b)dbdx = 2\pi b\, db\, N_o \frac{Z}{A} dx \tag{7}$$

where N_o is Avogadro's number (number of molecules/mole) and *Z* and *A* are the total charge/molecule (i.e., the number of electrons per molecule) and molecular weight of the material (i.e., the number of grams/mole, roughly the number of protons and neutrons in the molecule), respectively.

We now differentiate Eq. 6 and solve for *2b db*, obtaining in absolute value:

$$2b\, db = 2m_e c^2 \frac{z^2}{\beta^2} r_e^{\,2} \frac{dw}{w^2} \tag{8}$$

By combining Eqs. (7) and (8), we find the probability *dn(w)* for an energy loss *dw* in a track length *dx* of:

$$dn(w)dx = 2\pi\, m_e c^2 N_o \frac{Z}{A} r_e^{\,2} \frac{z^2}{\beta^2} \frac{dw}{w^2} dx = C \frac{z^2}{\beta^2} \frac{dw}{w^2} dx \tag{9}$$

where we have set $C = 2\pi\, m_e c^2 N_o \frac{Z}{A} r_e^{\,2}$. As the incident particle slows down just before it stops, it will pick-up (i.e., capture) electrons, thus decreasing its "effective charge". An empirical expression for this decrease is given by the Barkas expression for the effective charge:

$$z^* = z\,[1 - exp(-125\, z^{-2/3}\beta)] \tag{10}$$

so z^* should replace *z* in Eq. 9.

Eq. 9 is the Rutherford Scattering Formula. The quantity *dn(w)* can be interpreted as the *number of electrons* of energy *w* in *dw* emitted per unit track length. To obtain the total number of electrons emitted per unit track length, this expression is integrated from a minimum energy, say the mean ionization energy, *I*, in water (~ 69 eV) to the maximum transferrable energy to an

electron, which is $w_{max} = 2m_e c^2 \beta^2 \gamma^2$ with $\gamma^2 = (1 - \beta^2)^{-1}$, derivable from kinematic considerations applied to a head-on collision between the particle and an electron (assumed at rest). The total number of electrons emitted per unit track length in this approximation is:

$$n(z^*, \beta) = C \frac{z^{*2}}{\beta^2} \int_I^{w_{max}} \frac{dw}{w^2} = C \frac{z^{*2}}{\beta^2} \left| \frac{1}{I} - \frac{1}{w_{max}} \right| \qquad (11)$$

We note in particular that as far as the kinetics of the *incident particle* is concerned, the number of electrons emitted is a function only of z^{*2}/β^2 (and increases linearly with it) since for most energies of incoming particles, $w_{max} >> I$, so that $1/w_{max}$ can be neglected in Eq. 11.

We have gone through this *classical semi-quantitative* derivation to show the main features of the formula. In particular, it shows that for the approximations made, the number of electrons emitted per unit length is directly proportional to z^{*2}/β^2. Therefore, in particle energy regions where a quantitative biological effect is the same for any particle of a given z^{*2}/β^2, rather than a given LET, a better descriptor of biological effect in those energy regions depends on the *number of electrons (deltas) emitted per unit track length*, i.e., z^{*2}/β^2, rather than the total LET. We will come back to this in discussing biological effects as a function of particle track structure in Section 4.0.

3.2 The Amorphous Model of Charged Particle Tracks

A simple model to describe the decrease in energy deposition by electrons with distance away from the track trajectory, the *amorphous track* model, was introduced into radiobiology by Butts and Katz (1967) in studying the inactivation of dry enzymes and viruses by heavy ions. To obtain the way the absorbed energy density or "dose" decreased with distance from the track trajectory, they started with the Rutherford formula (Eq. 9) giving the number of delta rays per unit length of track having energies between w and $w + dw$ produced by a charged particle of effective charge z^*e moving with speed $v = \beta c$:

$$\begin{aligned} dn &= (Cz^{*2}/\beta^2)\, dw/w^2 \qquad && w \le w_{max} \\ dn &= 0 && w > w_{max} \end{aligned} \qquad (12)$$

where $C = 2\pi\, m_e c^2\, N_o \frac{Z}{A}\, r_e^2$ as before.

It can be shown in classical kinematics that electrons of energy w are ejected at an angle θ to the trajectory by the expression:

$$\cos^2\theta = w/w_{max} \qquad (13)$$

From equation (12), we see that most of the electrons have energies much less than w_{max} and so have ejection angles approximately equal to 90° to the track direction. Thus, in this model, the electrons are assumed to be ejected normal to the track trajectory.

Now consider the energy deposition pattern looking head-on into the particle track. We proceed by calculating the energy per unit volume deposited by the electrons knocked-out of

atoms of the medium by a charged particle of charge z^*e and mass m traveling at velocity βc. The number of electrons (per unit track length) traversing a cylindrical shell of thickness dt and radius t centered on the track trajectory is the number with energy between $w(t)$ and w_{max}:

$$n[w(t)] = \frac{Cz^{*2}}{\beta^2}\int_{w(t)}^{w_{max}} \frac{dw}{w^2} \tag{14}$$

The assumption is made that the electrons move in straight lines normal to the track trajectory. A further assumption is made here that the range-energy relation for the electrons is linear with electron energy ($t = kw$). This is valid (i.e., to within 10%) at energies below 2 keV. Then $dw = k^{-1}dt$ and for a cylindrical shell of thickness dt, the total energy deposited in the shell (per unit track length) is the number of electrons traversing the shell (per unit track length) times the energy deposited in the shell per electron. If the particle track length considered, Δx, is long enough for many electrons to be ejected and short enough that the velocity of the particle can be considered constant, the mean energy per unit mass (or "dose") in the cylindrical shell at a distance t from the trajectory can be obtained by calculating the total mean energy deposited by the delta electrons in the cylindrical shell divided by the mass of the shell (assumed here to be water):

$$\begin{aligned} D_\delta(t) &= \frac{n[w(t)]dw\Delta x}{2\pi t dt \rho_{water}\Delta x} = \frac{Cz^{*2}k^{-1}dt}{2\pi t dt \rho_{water}\beta^2}\left[\frac{1}{w(t)} - \frac{1}{w_{max}}\right] \\ &= \frac{Cz^{*2}}{2\pi t\beta^2}\left[\frac{1}{t} - \frac{1}{T_{max}}\right] \end{aligned} \tag{15}$$

where we have set ρ_{water}=1 g/cm^3 and $T_{max} = kw_{max}$. For $t<<T_{max}$, the second term can be neglected, and the "dose" falls off as the reciprocal of the square of the distance from the trajectory. The reason "dose" is in quotes here is that this term is appropriate only to regions where electronic equilibrium exists, a condition far from being fulfilled here.

Note that particles with the same z^{*2}/β^2 in this model have the same deposition patterns (close to the trajectory, i.e., where $t<< T_{max}$) caused by these delta rays. So to the extent that this model adequately describes track structure (i.e., the energy loss patterns) of high energy charged particles, and if biological effects depend mainly on this "close-in dose" caused by multiple delta rays (electrons) being knocked out of atoms as the particles slow down, biological effects might be expected to be the same for all high energy heavy charged particles with the same z^{*2}/β^2, and this quantity might be a good descriptor of biological effects for these particles. One implication of this model for biological effects, is that the longer range (single) delta rays from these tracks might be neglected. (See article here (Curtis, 2013) for a discussion of this conjecture).

4.0 Experimental Evidence of z^{*2}/β^2 as Descriptor of Biological Response

One of the first indications that LET might not be a good indicator of biological response in certain ranges of LET was pointed out by (Bewley, (1968**)** and (Barendsen *et al.*, 1966) in noting differences in survival of human T1 cells irradiated in the LET range between 100 - 400 keV/μm. Oxygen enhancement ratios[2] (OERs) in this LET range were higher for the heavy ions with z > 2 (Todd, 1966) than for Helium ions (i.e., alpha particles, z = 2) (Barendsen et al., 1966). It was pointed out (Curtis, 1970) that this might be due to the difference in *track structure* between the ion beams used in the two experiments. In Fig. 1, OER is plotted on the left for the two experiments against LET and against z^{*2}/β^2 on the right. The data overlap to a much greater extent on the right, and are consistent with lying on the same curve.

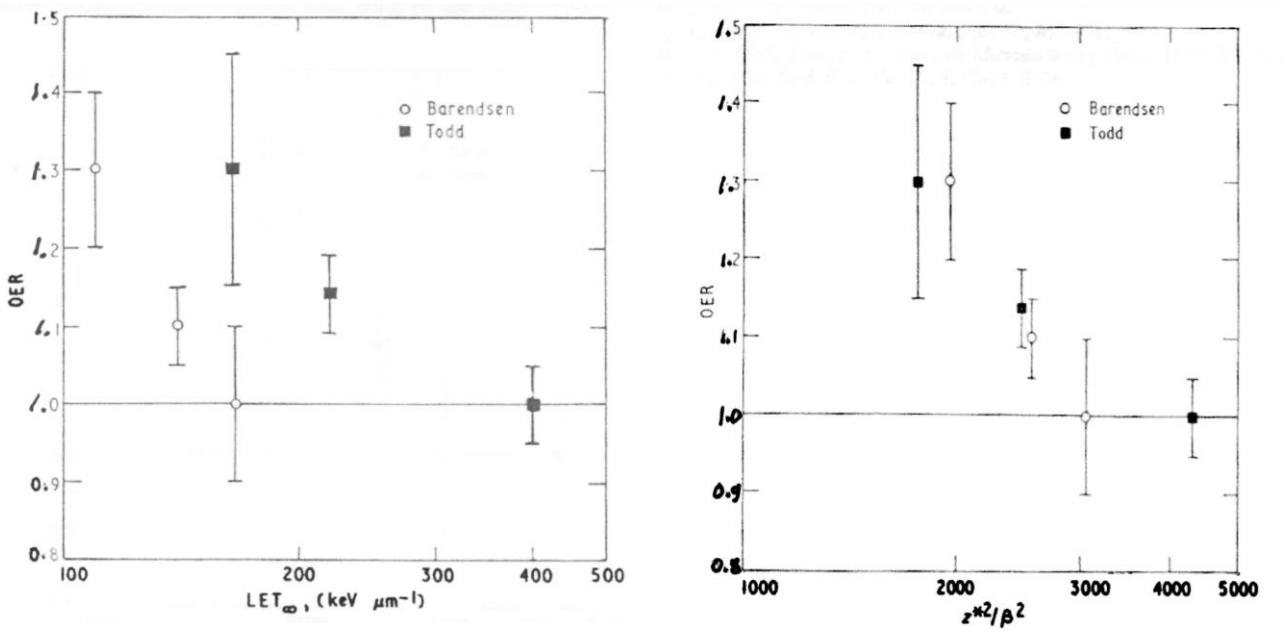

Fig.1. OER of human T1 cells plotted for alpha particles, z=2, (open symbols) and heavier ions, z > 2 (closed symbols) against LET_∞ on the left and against z^{*2}/β^2 on the right (Curtis, 1970).

This has been seen in other experimental cell systems as well, e.g., cell survival curves and Relative Biological Effectiveness ratios (RBEs) (Thacker *et al.*, 1979), (Blakely *et al.*, 1979), (Furusawa *et al.*, 2000). An example is shown in Figure 2 for cell survival of V79 and human T1 cells (Thacker *et al.*, 1979). Here we see again that there is a splitting of the curves when plotted against LET and convergence of the data when plotted against z^{*2}/β^2.

[2] The Oxygen Enhancement Ratio (OER) is the ratio of doses to produce the same survival of cells in the hypoxic and oxygenated conditions, i.e. D_{hyp}/D_{oxy} for equal survival.

In every case, heavier higher *z* ions produce higher energy deltas that scatter farther from the trajectory than the lower energy deltas from lighter lower *z* ions at the same LET. So at the same total energy lost per unit track length, there are more electrons at the lower energies being emitted per unit track length by the low-z ions to make up for the energy being lost to the higher energy electrons ejected by the higher energy high-z ions. Therefore, z^{*2}/β^2 (which is proportional to the *number* of electrons emitted per unit track length) is higher for lower *z* ions than higher *z* ions at the same LET and it is not surprising that this difference in track structure might be important in determining biological effects and that these effects would be higher for lower *z* ions.

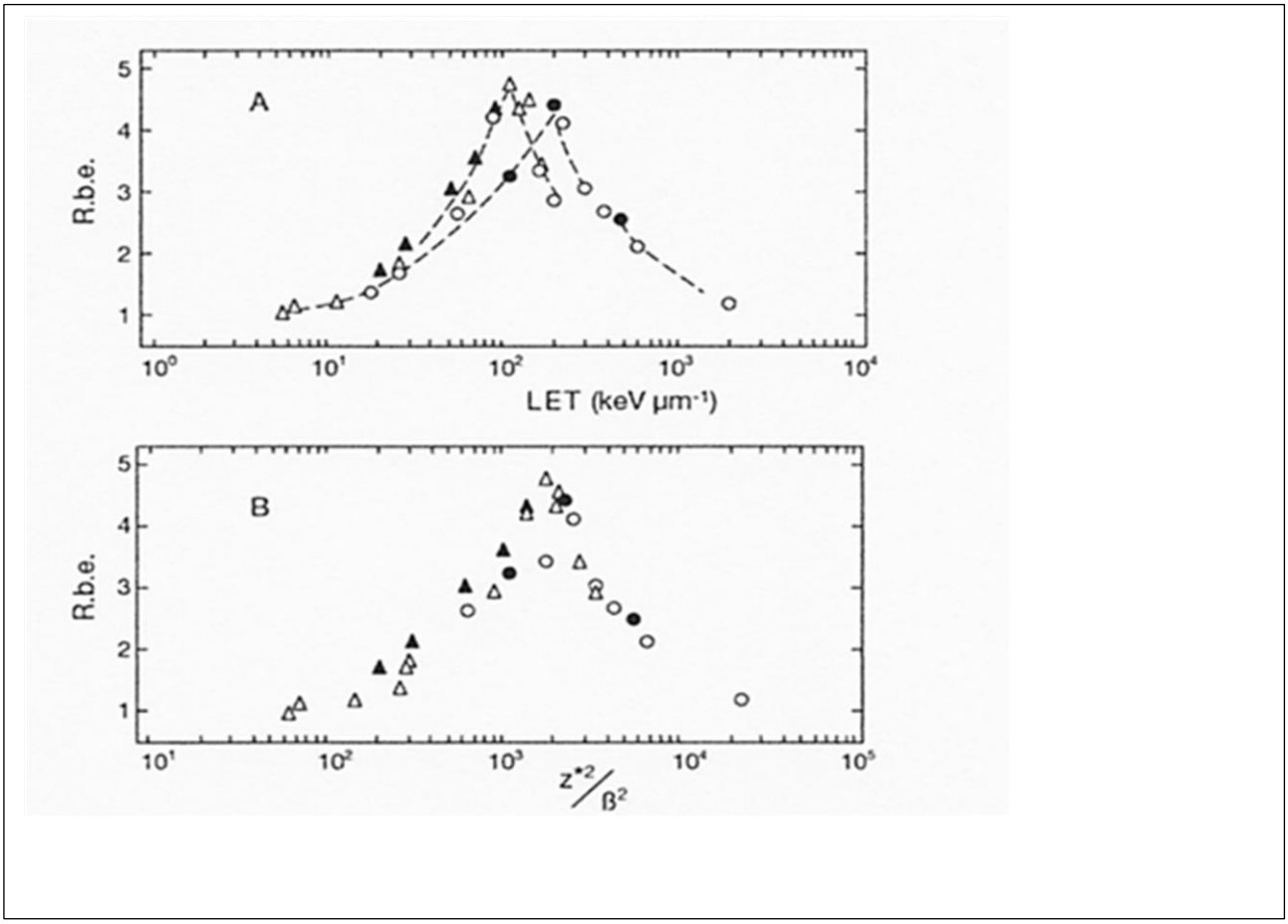

Fig.2. Cell survival RBEs for V79 cells (solid symbols) and human T1 cells (open symbols) plotted against LET in panel A and against z^{*2}/β^2 in panel B. (From Thacker et al, 1979).

5.0 Monte Carlo Calculations of Track Structure

So far these models have defined average or mean values of the quantities, such as "dose" as a function of distance from the track, and the *mean* number of electrons ejected per unit track length. As mentioned in Section 2.0, charged particle tracks are stochastic in nature so that biological targets within the body experience a distribution rather than a mean value of these quantities. This has led to a considerable effort in the field of microdosimetry to develop probabilistic (i.e., Monte Carlo) codes for dealing with this feature. Several articles on the history and techniques of Monte Carlo calculations can be found in this encyclopedia and have been referred to in Section 2.0.

The feature of the difference in track structure between various ions of the same LET is seen clearly in the Monte Carlo calculated tracks by the PARTRAC code developed by the group in Germany (Dingfelder et al, 1998). As an example of this, we show here two tracks, a helium ion (alpha particle, z = 2) and an iron ion (z = 26) at the same LET = 150 keV/μm. The animations show to scale, simulations of *segments* of tracks of the selected high-LET particles traveling through liquid water. The viewer is traveling at constant velocity parallel to (and in the same direction as) the moving particle, slightly ahead of it and viewing it over his/her right shoulder to see the developing track in perspective --- large interaction-point symbols are close by and they become smaller as they recede in the distance. Each track consists of a mapping of the inelastic interaction points of the primary particle and of the secondary delta-ray electrons it ejects. These animations were made available for display on this website by courtesy of Werner Friedland, Herwig Paretzke and Maximillian Kreipl (Kreipl et al, 2009).

The animations show two particles of very different charge and velocity but selected to have the *same LET* (150 keV/μm) for comparison of the different energy loss patterns from each. Figure 3 is for a 56 GeV ^{56}Fe ion, while Figure 4 is for a 2 MeV He-4 ion (i.e., an alpha particle). The specific energies are 1 GeV/nucleon for the Fe ion and 0.5 MeV/nucleon for the He ion.

Because of the low velocity of the He ion, its interactions with the water molecules can eject delta electrons of only very low energies. Hence the entire track is confined to a narrow cylindrical region of dense ionization close to the path of the He ion (within a few tens of nanometers at most). Due to energy loss, the (invisible) location of the primary particle stays behind the viewer in the course of the track. By contrast, the Fe ion has very high relativistic velocity and so can eject delta electrons up to high energies, which can travel far from the path of the Fe ion. As a consequence, the track structures, including the local ionization densities, are very different for the two ions, even though their LET (i.e. average energy deposition per unit path length) is the same. While all the energy lost by the He ion is deposited within a few tens of nanometers of the He ion's path, the Fe ion deposits less than 20% of its energy this close to the Fe ion's path --- the remaining 80% is carried away to greater distance by the higher-energy delta electrons. Some of these higher-energy electrons can be seen only by looking back at the track in the far distance.

All symbols in the animations represent point interactions of the primary ion or secondary electrons in the water medium. The symbols have been drawn as finite spheres to provide distance perspective to the simulations ---- the symbols are full sized when close to the

viewer and shrink proportionately as they fade into the distance. The key to symbols is as follows:

Dark blue sphere: An inelastic interaction of the primary ion (ionization, excitation or charge transfer);
Red sphere: An ionization interaction of an electron;
Light blue sphere: An excitation by an electron;
Olive sphere (He ion): Sub-excitation electron under thermalization; its tortuous path is replaced by straight movement towards its final position;
Green sphere: Locality of a hydrated electron after thermalization.

The time scale for each ion is different. The faster iron ion on the left will traverse the entire track segment in 16 femto seconds, while the slow helium ion on the right will traverse the same distance in 450 fs. The entire animation only lasts about three minutes. You may start and stop the animations, which run side-by-side, by simply clicking on the animation box.

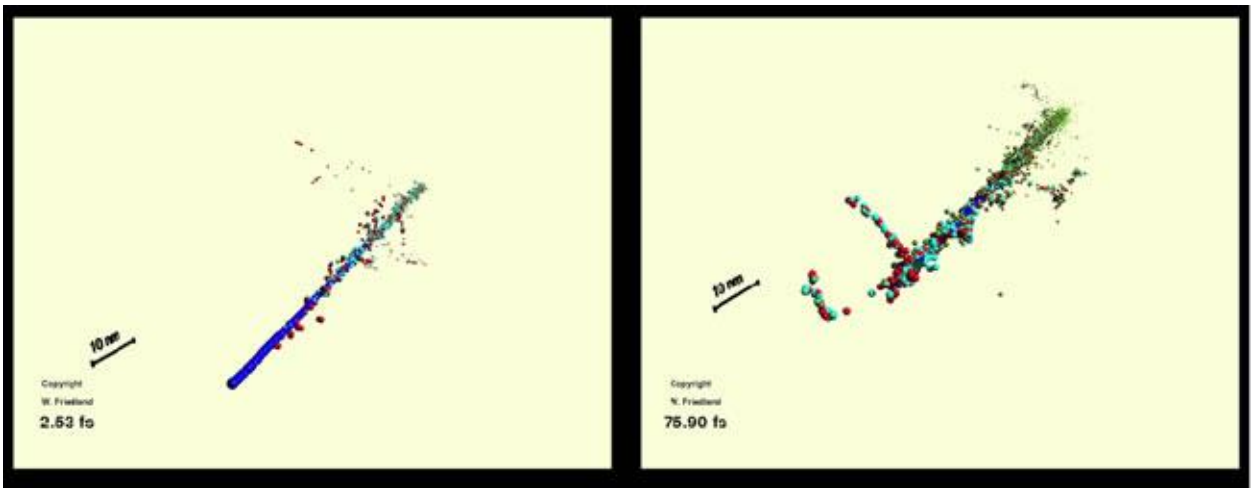

Fig.3. Monte Carlo simulation of a 1 GeV/amu Fe ion. The LET is 150 keV/μm.

Fig. 4. Monte Carlo simulation of a 0.5 MeV/amu He ion. The LET is 150 keV/μm.

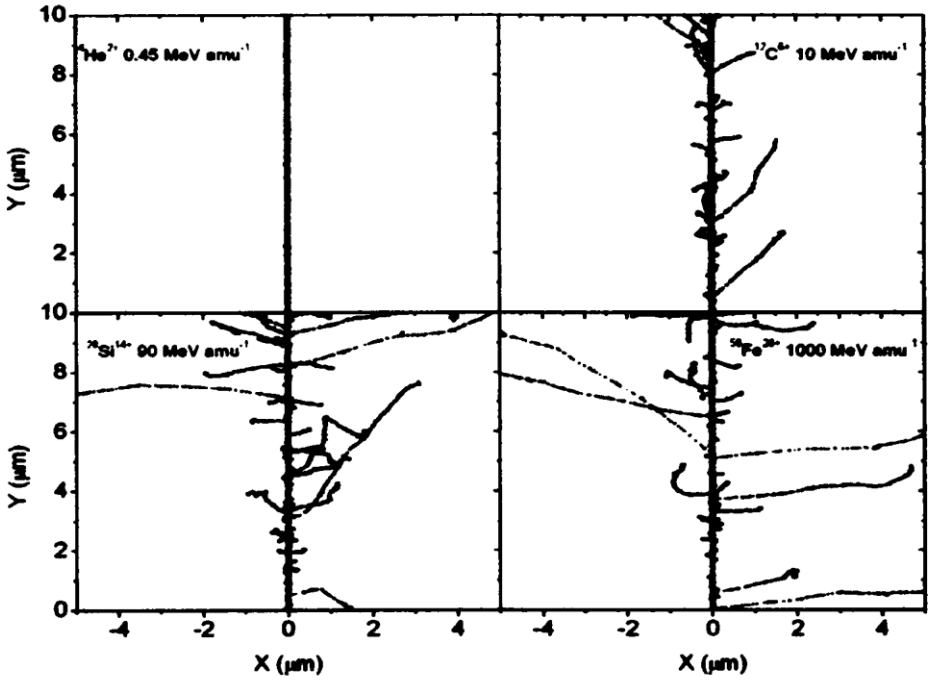

Fig.5. Projections over the XY-plane of simulated track segments of ^{4}He, ^{12}C, ^{28}Si, and ^{56}Fe ions at ~10^{-12}seconds. All have an LET of 150 keV/μm. Each dot represents a radiolytic species, $H^{\bullet}$, $^{\bullet}OH$, H_2, H_2O_2 or e^{-}_{aq} (Plante and Cucinotta, 2008).

Much work has been done in developing other Monte Carlo codes as well. A review has been published by Nikjoo, *et al*., (2006). Also available on the THREE website is RITRACKS, a Monte Carlo code developed at NASA by Plante and Cucinotta (2008) which simulates track segments of high energy heavy ions in liquid water. An example of output from this code is shown in Figure 5. The differences in track structure at this scale of 0–4 μm in water is clear, especially between the He, C and Fe ion tracks.

6.0 Incorporation of track structure into the NASA Space Radiation Risk Model

NASA has long recognized the inadequacy of LET for specifying biological effects from the various species of particles in the Galactic Cosmic Rays and the importance of track structure in developing its Space Radiation Risk Model (Cucinotta et al., 2013). The Risk of Exposure Induced Death (REID) and Risk of Exposure Induced Cancer (REIC) are both defined by functions that involve integrations over the fluence spectra of the particles times radiation risk cross sections, which are in turn functions of the z^{*2}/β^2 parameter. Risk cross section (the risk per unit fluence) is discussed in another article on this website (Curtis, 2013). Although much still needs to be done to refine the model and bring our increasing understanding of the dependence of the emergence of cancer on physical parameters such as z^{*2}/β^2 and fluence rate, a beginning has been made, and a growing understanding of the biological processes involved will ultimately bring down the uncertainties involved.

7.0 References

Barendsen, G.W., Koot, C.J., van Kersen, G.R., Bewley, D.K., Field, S.B., and Parnell, C.J., The effect of oxygen on impairment of the proliferative capacity of human cells in culture by ionizing radiations of different LET. Intern. J. Radiat. Biol. **10**, 317-327 (1966).

Bewley, D.K., A comparison of the response of mammalian cells to fast neutrons and charged particle beams, Radiat. Res. **34**, 446-458 (1968).

Blakely, E.A., Tobias, C.A., Yang, T.C., Smith, K.C. and Lyman, J.T., Inactivation of human kidney cells by high-energy monoenergetic heavy-ion beams, Radiat. Res. **80**, 122-160 (1979).

Braby, L.A., Microdosimetry and detector responses. https://three.jsc.nasa.gov/articles/Microdosimetry-Braby.pdf. Date posted: 02-06-14.

Butts, J.J. and Katz, R., Theory of RBE for heavy ion bombardment of dry enzymes and viruses, Radiat. Res. **30**, 855-871 (1967).

Cucinotta, F.A., Nikjoo, H., and Goodhead, D,A., Applications of amorphous track models in radiation biology, Radiat. Environ. Biophys. **38**, 81-92 (1999).

Cucinotta, F.A., Kim, M.-H.Y., and Chappell, L.J., *Space Radiation Cancer Risk Projections and Uncertainties – 2012*, NASA/TP-2013-217375 (2013).

Curtis, S.B., The effect of track structure on OER at high LET, *Charged Particle Tracks in Liquids and Solids, Conference Series **8***. London, England: Institute of Physics and the Physics Society, 140-142 (1970).

Curtis, S.B., The evolution of risk cross section. https://three.jsc.nasa.gov/articles/Risk_Cross_Section_Curtis.pdf. Date posted: 11-01-13.

Curtis, S.B., Fluence rates, delta rays and cell nucleus hit rates from galactic cosmic rays. https://three.jsc.nasa.gov/articles/tracksinspace.pdf . Date posted: 02-28-2013.

Dicello, J.F., Cucinotta, F.A., Interpreting microdosimetric spectra. https://three.jsc.nasa.gov/articles/MICRODOSIMETRY.pdf. Date posted: 12-10-2012.

Dingfelder, M., Hantke, D., Inokuti, M., and Paretzke H.G., Electron inelastic-scattering cross sections in liquid water. Radiat. Phys. Chem. **53**: 1–18 (1998).

Dingfelder, M., Monte carlo track simulations. https://three.jsc.nasa.gov/articles/monte-carlo-Dingfelder.pdf. Date posted: 02-06-2014.

Furusawa, Y., Fukutsu, K., Aoki, M., Itsukaichi,H., Eguchi-Kasai, K., Ohara, H., Yatagai, F., Kanai, T., and Ando, K., Inactivation of aerobic and hypoxic cells from three different cell lines by accelerated ^{3}He-, ^{12}C-, and ^{20}Ne-ion beams, Radiat. Res. **154**: 485-496 (2000).

Grahn, D., ed., *HZE Particle Effects in Manned Spaceflight*, National Academy of Sciences, Washington, DC, 1973.

Kreipl, M.S., Friedland, W. and Paretzke, H.G. Interaction of ion tracks in spatial and temporal proximity. Radiat. Env. Biophys. **48**: 349-359 (2009).

Nikjoo, H., Uehara,S., Emfietzoglou D. and Cucinotta F.A., Track-structure codes in radiation research. Radiat. Meas. **41**: 1052–1074 (2006).

Plante, I. and Cucinotta, F.A., Ionization and excitation cross sections for the interaction of HZE particles in liquid water and application to Monte Carlo simulation of radiation tracks, New J. of Phys. **10:** 125020 15pp (2008).

Rossi, B., *High Energy Particles*, Prentice-Hall, Inc., NJ, 1952.

Thacker, J., Stretch, A., and Stevens, M.A., Mutation and inactivation of cultured mammalian cells to beams of accelerated heavy ions. II Chinese hamster V79 cells, Int. J. Radiat. Biol. **36**: 137-148 (1979).

Toburen, L., Development of monte carlo track structure codes. https://three.jsc.nasa.gov/articles/Monte-Carlo-Track-Structure-Toburen.pdf. Date posted: 02-06-2014.

Todd, P.W., Reversible and irreversible effects of densely ionizing radiations upon the reproductive capacity of cultured human cells, Med. Coll. Virginia Quart. **1**, No. **4**, p. 2 – 14 (1966).